This is the last draft sent to the Editorial by the authors of the article:

M. GÓMEZ, P. VALLES, S. F. MEDINA

"Study of the microstructure and strain induced precipitation during thermomechanical processing of low carbon microalloyed steels"

Materials Science Forum
Volume 706-709, 2012, Pages 2118-2123
DOI: 10.4028/www.scientific.net/MSF.706-709.2118
ISSN: 0255-5476

Study of the microstructure and strain induced precipitation during thermomechanical processing of low carbon microalloyed steels

GÓMEZ Manuel[1, a], VALLES Pilar[2,b] and MEDINA Sebastián F.[1,c]

[1]National Center for Metallurgical Research (CENIM-CSIC), Avda. Gregorio del Amo 8, 28040 Madrid, Spain

[2]Instituto Nacional de Técnica Aeroespacial (INTA), Ctra. Torrejón-Ajalvir, Km.4. 28850 Torrejón de Ardoz, Madrid, Spain

[a]mgomez@cenim.csic.es, [b]vallesgp@inta.es, [c]smedina@cenim.csic.es

Keywords: Microalloyed steel; Pipeline; Thermomechanical processing; Acicular ferrite; Mechanical Properties; Transmission electron microscopy; Precipitation.

Abstract. A series of anisothermal multipass hot torsion tests were carried out to simulate hot rolling on three high-strength low-carbon steels with different amounts of Mn, Mo, Nb and Ti and designed for pipeline construction. Mean Flow Stress was graphically represented against the inverse of temperature to characterize the evolution of austenite microstructure during rolling. The effect of austenite strengthening obtained at the end of thermomechanical processing on the final microstructure obtained after cooling was studied. Higher levels of austenite strengthening before cooling promote a refinement of final microstructure but can also restrict the fraction of low-temperature transformation products such as acicular ferrite. This combined effect gives rise to a wide range of final microstructures and mechanical properties depending on the composition, processing schedule and cooling rates applied. On the other hand, the precipitation state obtained at diverse temperatures during and at the end of hot rolling schedule was evaluated by means of transmission electron microscopy (TEM) in two microalloyed steels. It was found that two families of precipitates with different morphology, composition and mean size can coexist in microalloyed steels.

Introduction

In response to the increasing demand of sources of energy such as oil and natural gas, the steel industry is developing low carbon microalloyed steels for pipeline applications whose microstructure provides an outstanding combination of properties. These steels include a strict combination of alloying and microalloying elements to obtain good formability, high weldability, adequate strength in corrosive environment and a precise balance of microconstituents in order to achieve excellent mechanical properties of strength and toughness at a reduced cost [1-3]. To obtain an adequate fine-grained final microstructure, the strict control of thermomechanical processing and accelerated cooling is also crucial [4-6]. Depending on the thermomechanical processing conditions and chemical composition, pipeline steels can present different microstructures. Several authors have found that the microstructure of acicular ferrite usually provides an optimum combination of mechanical properties [7-9]. Compared to a microstructure of polygonal ferrite, acicular ferrite contains higher density of dislocations and sub-boundaries, which is beneficial to the strength. At the same time, cleavages in an acicular ferrite pipeline steel experience more bent paths and absorb more energy at low temperatures [3]. The formation mechanism of acicular ferrite provides a refinement of the mixed microstructure that improves strength and toughness [10].

The environment for acicular ferrite formation in hot rolled pipeline steels is quite different from that of welds, as nonmetallic inclusions acting as nucleation sites inside the austenite grains are extremely restricted in these steels. In pipeline steels, an increase in the amount of hot-deformation in the austenite non-recrystallization region during thermomechanical processing increases the volume fraction of acicular ferrite after cooling at the expense of bainitic ferrite. This results from

the higher density of substructure and dislocations within the austenite grains, which increases the nucleation rate of acicular ferrite [8,11,12]. On the other hand, it is known that the refinement of ferritic microstructure is enhanced by a fine-grained austenite before transformation, and especially by a microstructure of strengthened austenite with elongated grains, high dislocation density and ledges in the grain boundaries that increases the density of nucleation sites and promote high nucleation rates for ferrite [4,13]. In relation to this matter, this work studies the effect of austenite strengthening at the end of thermomechanical processing on phase transformation and final microstructure after cooling of three low carbon steels. On this purpose, the measurement of the parameter known as accumulated stress [14] is combined with metallographic observations. Besides, hardness measurements are used to approximate the strength properties of the steels for different deformation and cooling conditions.

On the other hand, it is known that strain-induced precipitates formed by microalloying elements and interstitials play a very important role on the microstructure evolution and final mechanical properties of steels with different final microstructures [7,15,16]. Precipitation state at different stages of thermomechanical processing of two microalloyed steels is also studied in this paper. For this goal, samples obtained by means of quench-interrupted hot rolling simulations were observed.

Materials and Experimental Procedure

Three low carbon steels were studied. As Table 1 shows, steel 1 is a CMn steel whereas steel 2 is a Nb-microalloyed steel. Both steels have a very low Ti%. Steel 3 is a low-carbon, high-Mn (Nb, Ti)-microalloyed steel with higher Mo, Ni and Cu additions. All steels have similar hardenabilities.

A series of rolling simulation tests were carried out in a computer-controlled hot torsion machine, on specimens with a gauge length of 50 mm and a diameter of 6 mm that were protected against oxidization with an argon flow. Relatively complex multipass hot-torsion schedules were designed to simulate a near-to-industrial hot rolling process. Prior to the simulation tests, the specimens were austenitized at a temperature of 1150 ºC for 15 min. The temperature was then lowered to that corresponding to the first deformation pass, which was 1125 ºC. The simulations consisted of the performance of 16 or 17 passes following the schedules shown in Table 2. The schedule was divided in three phases and it was designed to achieve full recrystallization in Phase 1 at high temperatures and austenite strengthening by partial or no recrystallization during Phases 2 and 3. Phases 1 and 2 were common to all tests and all steels. A long time interval with a strong temperature step between Phases 1 and 2 ensured that last finishing passes are applied within the pancaking domain. To study the influence of austenite strengthening on final microstructure, the strain applied during Phase 3 (i.e. at lower temperatures, close to phase transformation) took three different values (Phases 3a, 3b, 3c in Table 2). Doing so, the magnitude known as accumulated stress ($\Delta\sigma$) [14] attained three different levels at the end of hot rolling. The effect of austenite strengthening (value of $\Delta\sigma$) on final microstructure was assessed in two sets of samples. These samples were respectively water-quenched or slowly cooled in an argon flow (at approximately 3.5 ºC/s) from 750 ºC, after applying the corresponding deformations in Phase 3. The samples were prepared by metallographic techniques and microstructures were observed by optical microscopy on a longitudinal surface of the specimens at 2.65 mm from the axis, after etching with 2% nital. Vickers Microhardness values were measured on the samples quenched or cooled from 750 ºC according to UNE-EN ISO 6507-1 standard using a load of 5 kgf.

Table 1. Chemical composition of steels studied (mass%).

Steel	C	Si	Mn	S	P	Al	Mo	Ni	Cu	Cr	Nb	Ti	N
1	0.056	0.31	2.43	<0.001	0.003	0.046	<0.005	<0.005	0.001	<0.005	<0.001	0.007	0.0022
2	0.053	0.33	2.45	<0.001	0.002	0.037	<0.005	<0.005	0.002	<0.005	0.046	0.007	0.0025
3	0.056	0.31	1.90	0.0015	0.011	0.029	0.213	0.221	0.193	0.044	0.046	0.018	0.0044

Table 2. Hot torsion rolling simulation schedules carried out in the study.

Phase	Pass number	Pass strain			Interpass time (s)	Temperature (°C)
Reheating						1150×15 min
1	1-11	0.1			10	1125-1075
Interval 1-2 (410 s)						
2	12-15	0.3			10	870-810
Interval 2-3 (60 s)						
		Steel 1	Steel 2	Steel 3		750
3a (low $\Delta\sigma$)	16	0.20	0.05	0.1		750
3b (medium $\Delta\sigma$)	16	0.30	0.12	0.25		750
3c (high $\Delta\sigma$)	16	0.30	0.30	0.3	5	760
	17	0.20	0.15	0.3		750

In order to characterize the evolution of precipitation state during hot rolling, several samples of steels 2 and 3 were water-quenched from different temperatures along the hot rolling simulation schedules. The characteristics (morphology, nature, mean size) of the precipitates were determined by transmission electron microscopy (TEM), using the carbon extraction replica technique. The replicas were taken at 2.65 mm from the axis. Energy dispersive X-ray (EDX) analysis was carried out to characterize the chemical composition of the particles observed.

Results and Discussion

The torsion test gives the values of torque applied versus the number of turns made on the specimen, which are transformed respectively into equivalent stress and strain using Von Mises criterion [17]. The microstructural evolution of steel during hot rolling is usually studied on the curves of Mean Flow Stress (MFS) versus the inverse of temperature. MFS is determined in each step by dividing the area below the stress-strain curve by the strain applied [18]. In Fig. 1 it is possible to see three different zones. The first zone (1) corresponds to roughing deformations at high temperatures, where MFS grows as temperature decreases. Austenite recrystallizes completely between passes and the increase in stress is due only to the decrease in temperature. After an interphase cooling interval, the second zone of the curve (phase 2) shows higher values of stress due to the higher values of pass strain applied. Besides, an increase in the slope can be observed, which denotes a greater tendency towards hardening due to the incomplete recrystallization of austenite between finishing passes. This strengthening can be quantified by the magnitude known as accumulated stress ($\Delta\sigma$) [14]. In Phase 3, the rolling schedule has been modified to obtain different levels of final strengthening (three values of $\Delta\sigma$), as seen in Fig. 1 for Steel 2. In certain cases, a decrease in MFS can be observed, as a result of lower values of pass strain applied in Phase 3 and also the partial restoration of austenite during cooling interval between Phases 2 and 3 [19].

Figure 2 shows the microstructure of the three steels after quenching or cooling from 750 ºC for two levels of austenite strengthening at the end of hot rolling. It can be seen that the microstructure is much finer for the case of microalloyed steels (2 and 3), compared to the CMn steel 1. On the other hand, as can be expected, fast cooling rates usually generate finer and more acicular microstructures. Acicular ferrite can be formed in X70-X80 steels even at cooling rates near 75 ºC/s [8]. Finally, the effect of strengthening state of austenite at the end of hot rolling is more complex. In principle, higher levels of hot deformation introduce a higher density of ferrite nucleation sites and help to refine final microstructure [4,13], which is known to be beneficial for the balance of mechanical properties. However, it can be also observed at slow cooling rate and especially after quenching that the morphologies of acicular ferrite obtained for lower values of $\Delta\sigma$ are replaced by finer and more equiaxed ferrite grains when austenite is more severely deformed in the last rolling passes. The higher density of substructure and dislocations in heavily deformed austenite displaces

the transformation products from bainitic microstructures to acicular ferrite firstly [8] or even to polygonal ferrite and pearlite for slower cooling rates or low hardenabilities [11,12].

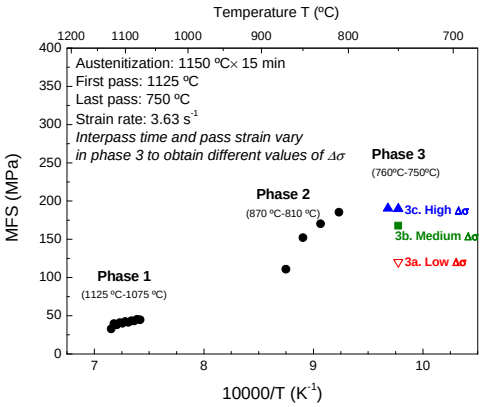

Figure 1. MFS versus the inverse of absolute temperature according to the schedules shown in Table 3. Steel 2.

Steel	Quench		Argon cooling	
	Low Δσ	High Δσ	Low Δσ	High Δσ
1	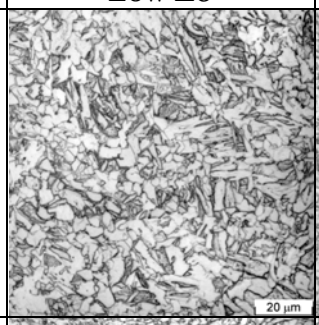	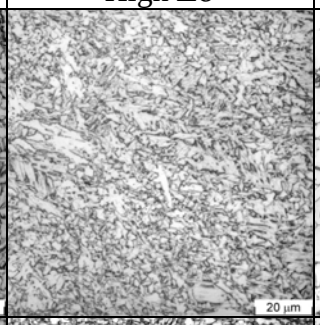	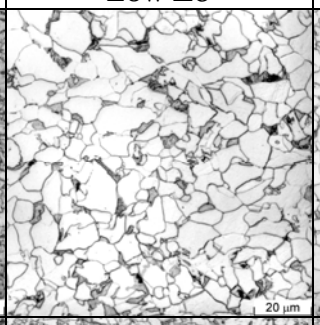	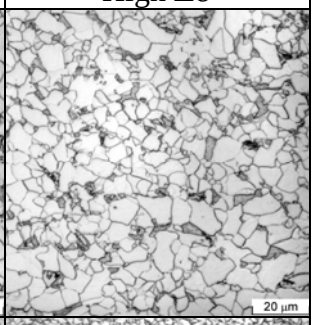
2	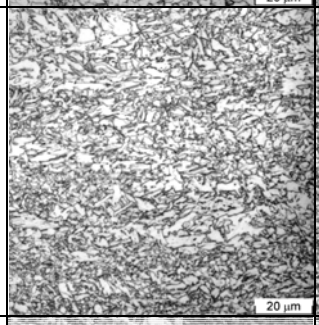	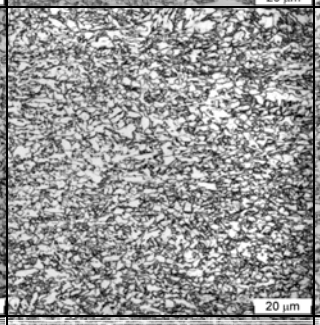	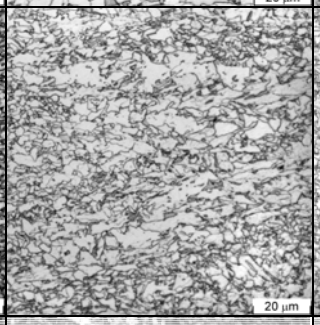	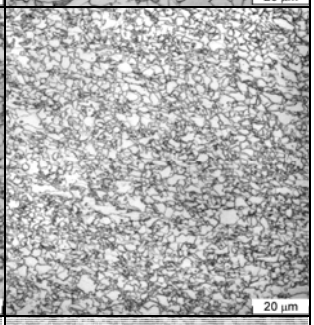
3	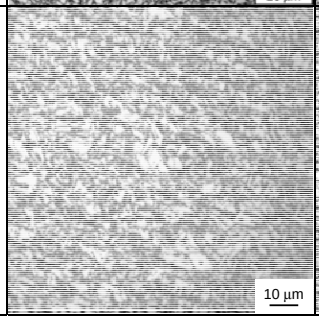	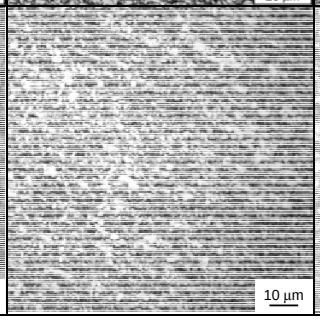	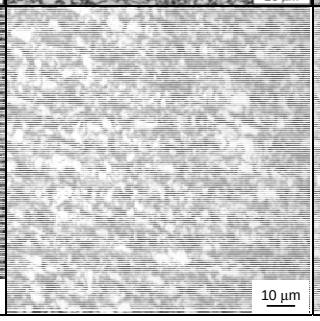	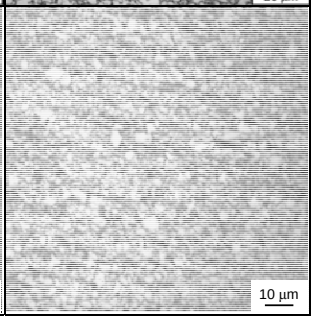

Figure 2. Microstructure of the three steels after quenching or slow cooling from 750 ºC for two different levels of austenite strengthening at the end of hot rolling.

In each steel, mechanical properties will vary depending on the deformation and cooling conditions that influence the final microstructure. Hardness values were measured in order to estimate the yield strength properties by means of empirical formulae [19]. Fig. 3 shows that the hardness of the samples of TiNbMo-microalloyed steel 3 decreases for increasing values of Δσ and

this happens with a similar trend for both cooling rates. Correspondingly, higher strength can be expected in the steel when austenite is less severely deformed in the last passes just before final cooling. This can be explained by the transition from the acicular ferrite microstructure present in the sample with low $\Delta\sigma$ to the more equiaxial morphology obtained for high $\Delta\sigma$, despite the simultaneous refinement of microstructure observed. Nb-microalloyed steel 2 presents slightly lower hardness values than steel 1 and not very different trend versus cooling and $\Delta\sigma$. On the other hand, it can be observed that CMn steel 1 offers considerably lower values of strength in slowly cooled samples as a result of the coarser and equiaxed ferritic microstructure observed in Fig. 2. However, the sample that was quenched from heavily deformed austenite kept a microstructure of relatively acicular ferrite with enhanced grain refinement. This microstructure generated strength values comparable to those obtained in microalloyed steels under these particular conditions.

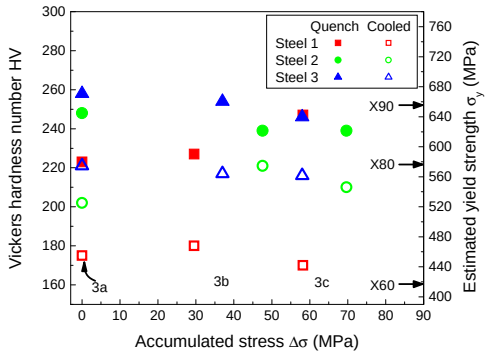

Figure 3. Values of Vickers Microhardness (HV) as a function of accumulated stress ($\Delta\sigma$) obtained at the end of hot rolling simulation. HV was measured on quenched or cooled samples of the three steels after following hot rolling simulation schedules 3a, 3b and 3c shown in Table 2. On the right axis, yield strength values are estimated as σ_y = 2.6 HV [19] and the specified minimum yield strengths (SMYS) for several steel grades are indicated.

Finally, the precipitation state was studied in steels 2 and 3. (Ti, Nb) carbonitrides with mostly cuboidal shapes were observed after reheating. These particles had lower Ti content in steel 2. Table 3 shows the theoretical solubility temperatures calculated for carbonitrides, nitrides and carbides [20]. According to these values, a certain fraction of undissolved TiN particles will remain after reheating in all cases, even for steels 1 and 2, as the residual Ti content (0.007%) is high enough to cause TiN precipitation. Besides, the presence of undissolved Nb carbonitrides can be expected, as the solubility temperature for these precipitates is close to the reheating temperature. In steel 3, TiNbCN particles kept a mean size near 25 nm from reheating to the end of hot rolling. These precipitates had higher ratios of Nb and C and rounder shapes for decreasing rolling temperatures and occasionally they contained Mo. A second family of very fine round precipitates nucleated in steel 3 within the cooling step between roughing and finishing phases, i.e. between 1075 ºC and 870 ºC. These particles were identified as Ti-free, complex Nb carbonitrides where Mo is introduced in the lattice. They kept a nearly constant mean size of about 5 nm throughout hot rolling. Fig. 4a shows both types of precipitates of Steel 3 at the beginning of Phase 2. Regarding Steel 2, it also presented a second group of very fine Nb-rich carbonitrides at the end of Phase 2, as Fig. 4b shows.

Table 3. Calculated solubility temperatures (ºC) for the steel studied [20].

Steel	$NbC_{0.87}$	NbN	$NbC_{0.7}N_{0.2}$	TiC	TiN
1	---	---	---	864	1273
2	1062	1040	1102	860	1282
3	1068	1083	1116	945	1389

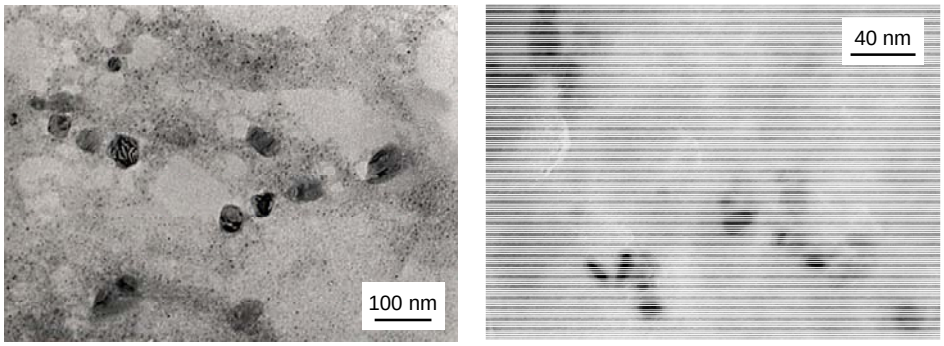

a) **b)**

Figure 4. TEM images showing two examples of precipitation state during hot rolling simulation schedule. "Td" means temperature of the last deformation applied and "Tq" means quenching temperature. **a)** Steel 3. Coarser and finer precipitates at the beginning of Phase 2, Td = 1075 ºC, Tq = 870 ºC; **b)** Steel 2. Fine precipitates at the end of Phase 2, Td = Tq = 810 ºC.

Conclusions

The final microstructure of acicular/equiaxial ferrite in low-carbon microalloyed steels is strongly influenced by thermomechanical processing and accelerated cooling conditions. As a result, it has been found that a CMn steel can reach similar values of strength to those obtained in more complex microalloyed steels under certain conditions. On the other hand, it has been found that two families of precipitates with different composition and mean size can coexist in studied microalloyed steels.

References

[1] K. T. Corbett, R. R. Bowen, C. W. Petersen, Int. J. Offshore Polar Eng. 14 (2004) 75–80
[2] I. D. S. Bott, L. F. G. De Souza, J. C. G. Teixeira, P. R. Rios, Metall. Mater. Trans. A 36A (2005) 443-454.
[3] W. Wang, Y. Shan, K. Yang, Mater. Sci. Eng. A 502 (2009) 38–44.
[4] T. Schambron, A. W. Phillips, D. M. O'Brien, J. Burg, E. V. Pereloma, C. C. Killmore, J. A. Williams, ISIJ Int. 49 (2009) 284–292
[5] J. Y. Koo, M. J. Luton, N. V. Bangaru et al., Int. J. Offshore Polar Eng. 14 (2004) 2–10.
[6] C. I. Garcia, K. Cho, M. Hua, A. J. DeArdo, Mater. Sci. Forum 638-642 (2010), 124–129.
[7] M.-C. Zhao, K. Yang, Y.-Y. Shan, Mater. Lett. 57 (2003) 1496–1500.
[8] Y. M. Kim, H. Lee, N. J. Kim, Mater. Sci. Eng. A 478 (2008) 361–370.
[9] Y. Smith, A. Coldren, R. Cryderman, Met. Sci. Heat Treat. 18 (1976) 59–65.
[10] S. Y. Shin, S. Y. Han, B. Hwang, C. G. Lee, S. Lee, Mater. Sci. Eng. A 517 (2009) 212–218.
[11] F.-R. Xiao, B. Liao, Y.-Y. Shan, G.-Y. Qiao, Y. Zhong, C. Zhang, K. Yang, Mater. Sci. Eng. A 431 (2006) 41–52
[12] P. P. Suikkanen, J. I. Kömi, L. P. Karjalainen, Met. Sci. Heat Treat. 47 (2005) 507–511.
[13] S. F. Medina, M. Gómez, E. Rodríguez, L. Rancel, ISIJ Int. 48 (2008) 1263–1269.
[14] M. Gómez, L. Rancel, B. J. Fernández, S. F. Medina, Mater. Sci. Eng. A 501 (2009) 188–196.
[15] M. Gómez, S. F. Medina, P. Valles, ISIJ Int. 45 (2005) 1711–1720.
[16] S. Shanmugam, N. K. Ramisetti, R. D. K. Misra, J. Hartmann, S.G. Jansto, Mater. Sci. Eng. A 478 (2008) 26–37.
[17] A. Faessel, Rev. Métall. Cah. Inf. Tech. 33 (1976) 875–892.
[18] F. H. Samuel, S. Yue, J. J. Jonas, B. A. Zbinden, ISIJ Int. 29 (1989) 878–886.
[19] M. Gómez, P. Valles, S. F. Medina, Mater. Sci. Eng. A 528 (2011) 4761–4773.
[20] E. T. Turkdogan, Iron Steelmaker 16 (1989) 61–75.